SOME CONSIDERATIONS ON GLOBAL AND LOCAL THERMAL COMFORT BASED ON FIALA‘S THERMAL MANIKIN IN THESEUS-FE

Stefan Paulke, Stefan Wagner

P+Z Engineering GmbH, Anton-Ditt-Bogen 3, 80939 München, Germany

s.paulke@puz.de (Stefan Paulke)

Abstract

Thermal management topics like air-conditioning and thermal comfort become more and more important during vehicle development. As a consequence the need for suitable tools and methods to predict the human comfort behaviour in cabins increases rapidly. THESEUS-FE is a finite element based software tool that realizes a fully coupled implementation of Fiala’s thermal sensation manikin presented in [1]. This paper will demonstrate the finite element based realization of the new manikin FIALA-FE in an existing solver environment. Various thermal comfort topics will be discussed in a second step. We will talk about the application of the finite element theory on the complete framework of formulas that represents the thermoregulatory human system. Because the major challenge for us was not to do a numerical solution of the bio heat equation based on the finite difference method, as shown in [1], but on a method that allows us to create our own finite element type, representing a single human material layer. Finally this paper will discuss different aspects of global and local thermal comfort prediction, based on mathematical models from literature. Using simulated skin and cloth temperatures the idea of the ‘equivalent temperature’ will lead us finally to a quite simple-to-use method of assessing local thermal comfort at given boundary conditions, typical for a vehicle simulation. Considering not only surface-to-surface radiation and convection but also sun radiation, seat contact and evaporation the equivalent temperature can then be derived at each body element sector of a thermal manikin.

Keywords: Thermal Manikin, Thermal Comfort Prediction, Finite Element Method.

Presenting Author’s biography

Stefan Paulke. Fished his civil engineering studies at the Technical University of Munich in 1997. From 1997 until 2001 he worked as a scientific assistant at the chair of Technical Mechanics, University of the Armed Forces in Munich, and finished his PhD thesis on thermo-mechanical coupling effects in 2001. Afterwards he started working at P+Z Engineering as a CAD Engineer. One year later he started with the THESEUS-FE project and is today responsible for technical stuff of this commercial software tool. In 2006 and 2007 he did the realization of the new thermal manikin FIALA-FE.

1 General

The manikin FIALA-FE (as a new feature of the software tool THESEUS-FE) provides all the thermo-physiological effects of the human body model published in the frequently cited PhD thesis [1] of 1998. D. Fiala supported our team frequently during the implementation of his theories. After many months of debugging and validation the results for the manikin computed with THESEUS-FE reached a good fit with the huge number of diagrams shown in literature.

From a mathematical point of view, the human organism can be separated into two interacting systems of thermoregulation: the controlling active system and the controlled passive system. The active system is simulated by means of cybernetic models predicting regulatory responses, i.e., shivering, vasomotion, and sweating, as discussed in [1]. The passive system is modelled by simulating the physical human body and the heat transfer phenomena occurring in it and at its surface. The physical body consists of body elements that are approximated as cylinders or sphere (head), they are separated into sectors and subdivided into material layers: skin, fat, muscle, bone.

Fiala`s advanced manikin combines both, the passive and active system, in a very complex model that reaches a good fit towards field measurements of human thermal responses in a wide range of environmental conditions. Some hundred of physical parameters that build up the standard humanoid (see table 2 in [2]) represent an average human. This is the manikin THESEUS-FE works with by default, but it is also possible for the user to build his own manikin with an arbitrary number of body elements, sectors and layers. E.g. it is thinkable to create fingers, nose and ears as new body elements, therefore reasonable physical parameters have to be extracted from literature or measurements.

In a transient coupled simulation, the manikin FIALA-FE permanently interacts with its environment via convection, evaporation, radiation and contact. Convective heat exchange typically takes place between the manikin outer surface and the surrounding airzones[1]. Evaporative heat loss on the skin results from a certain steam mass flow that raises the absolute humidity of the airzones, with distinctive mass flow rates due to sweating in a hot environment. The user defined contact regions might lead to additional heat conduction, e.g. between the upper legs and the seat. Sun radiation can be considered as well as thermal radiation between manikin surfaces and the surrounding structures via viewfactors, pre-calculated with the shell model shown in … . The total number of manikins of the new type “FIALA-FE” used in one transient fully coupled analysis is unlimited and the comparable small number of additional degrees of freedom (about 500 per manikin) will not lead to a serious rise in CPU time.

[1] In THESEUS-FE an ‘airzone’ is a air-steam mixture with two degree of freedom: temperature and humidity. In many thermal simulations an airzone typically represents the inner cabin air volume of a vehicle.

2 Fiala’s Passive System

2.1 Discretization

As shown in Fig. 1 THESEUS-FE uses two different models for the new manikin FIALA-FE. A shell model used during pre- and post-processing in the GUI to apply boundary conditions, define clothing, assign body parts or to visualize field results, e.g. skin or cloth temperatures.

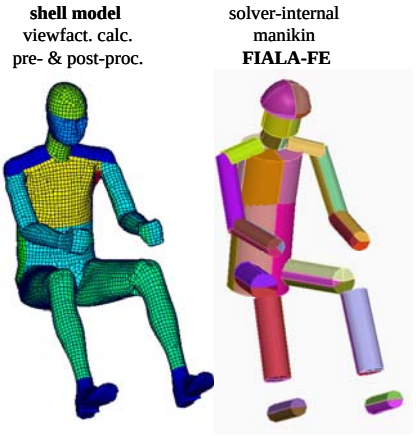

Fig. 1 Manikin representations.

A solver-internal manikin model FIALA-FE is based on the ideas of D. Fiala, who presented such a model in table 2 in [2]. This model uses a half sphere for the head and cylindrical solid bodies for the rest of the humanoid, as shown in Fig. 2 .

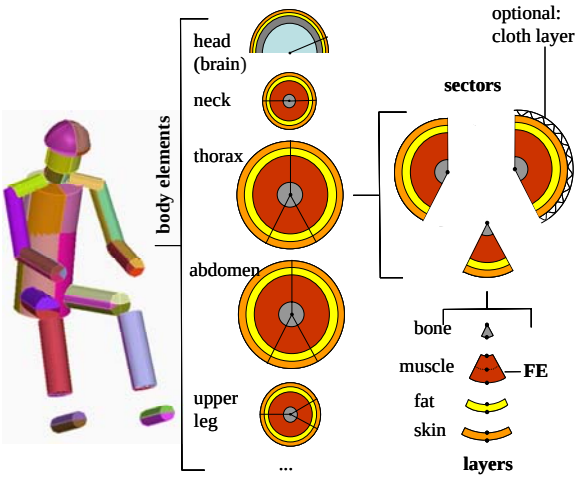

Fig. 2 Manikin discretization.

Both models are linked via heat fluxes that are first calculated on the shell model and then given to the

solver-internal manikin. To simulate the human heat conduction that transports metabolic heat from the inner regions to the outer skin or cloth surfaces FIALA-FE uses special finite elements (FE) that build up the layers, sectors and body elements as shown in Fig. 2. These elements provide not only temperature approximation functions for radial heat conduction but also arterial blood heating and special links to the blood pool temperature.

2.2 Bio Heat Equation

State of the art modelling of heat transport mechanisms in living tissues uses the bio heat equation. This partial differential equation states that the internal energy changes at each material point results from radial conduction, metabolism and arterial blood heating effects:

$$\underbrace{k\left(\frac{\partial^2 T}{\partial r^2}+\frac{\omega}{r}\frac{\partial T}{\partial r}\right)}_{\text{conduction}}+\underbrace{q_m}_{\text{metabol.}}+\underbrace{\rho_{bl}w_{bl}c_{bl}\left(T_{bl,a}-T\right)}_{\text{arterial blood heating}}=\rho c\frac{\partial T}{\partial t} \quad (1)$$

with the specific mass ρ, the specific heat c, the temperature T, the time t, the conductivity k, the body element radius r, the metabolic heat q_m , the specific mass ρ_{bl} of blood, the blood perfusion rate w_{bl} , the specific heat c_{bl} of blood, and the arterial temperature $T_{bl,a}$. The dimensionless parameter ω is 1 for cylindrical body elements (leg) and 2 for spherical body elements (head). The heat conduction is only considered in a radial direction, considering only temperature derivation along r. The equation describes the law of energy conservation at each material point of a layer that might represent skin, fat, muscle, bone, brain etc.

The magnitude of the physiological variables q_m and w_{bl} are affected by responses of the active system, as shown in [1] and [3]. The metabolic heat source q_m collects influences from different human phenomena: the basal metabolism, working, shivering and Q10-effect. The metabolic heat typically reaches high basal values at the brain and the abdomen core. Additional metabolism from working and shivering appears at muscle layers.

The arterial blood temperature $T_{bl,a}$ arises from the actual overall thermal state of the body and results from simulating the human blood circulatory system, as shown in [1]. Arterial and venous blood temperatures can be derived for each body element of the humanoid. The blood pool temperature appears as an additional degree of freedom of each manikin, representing the temperature of the blood leaving the human heart.

For a numeric solution of the partial differential equation (1) THESEUS-FE uses finite elements specially developed for this type of problem.

2.3 Human Heat Exchange with the Environment

Most heat of a humanoid is lost through the body surfaces[2]: radiation, convection, skin evaporation and contact heat fluxes will be considered in THESEUS-FE.

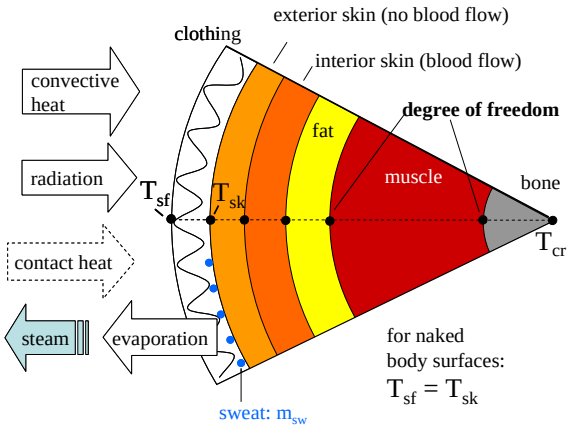

Fig. 3 Surface bound. cond. (hot environment).

All these different kinds of boundary conditions are visualized in Fig. 3, acting on a body element sector, e.g. upper leg anterior.

2.3.1 Contact

If the user defines contact for a body element sector heat conduction with the contact partner (e.g. the car seat) takes place at the outer surfaces and all other types of boundary conditions will be switched off automatically.

2.3.2 Convection

Convective heat exchange between a body surface area A_{sf} of temperature T_{sf} and the ambient air of temperature T_a considers both free (natural) and forced convection using combined convection coefficients $h_{c,mix}$

$$Q_{conv} = A_{sf}h_{c,mix}\left(T_a - T_{sf}\right) \quad (2)$$

For this coefficient D. Fiala uses a well validated analytical function from literature:

$$h_{c,mix} = \sqrt{a_{nat}\sqrt{\left|T_a - T_{sf}\right|} + a_{frc}v_{a,eff} + a_{mix}} \quad (3)$$

That depends on the location on the body, the surface and air temperature, and the effective airspeed $v_{air,eff}$ (m/sec). The coefficients $a_{nat,j}$, $a_{frc,j}$ and $a_{mix,j}$ are listed in table 2 in [2]. They have been derived from experiments and provide different values for each body element.

[2] A much smaller part of the total heat exchange takes place by respiration. THESEUS-FE considers this phenomenon too, as described in [1], [2] and [5].

2.3.3 Radiation

In a coupled simulation THESEUS-FE derives radiation heat fluxes for the shell model (Fig. 1, left) and applies them on body element sectors of the internal manikin model (FIALA-FE). The following radiation phenomena might be considered:

- radiation heat from sun
- transmission (e.g. through car glass)
- View-factor radiation (black- or grey-body)

In an uncoupled simulation the user defines a fixed radiation wall temperature T_w. The black-body approach leads then to

$$Q_{rad} = A_{sf} h_r (T_w - T_{sf})$$
$$h_r = \sigma \varepsilon_{sf} \varepsilon_w \psi_{sf-w} (T_{sf}^2 + T_w^2)(T_{sf} + T_w) \quad (4)$$

using absolute temperatures in Kelvin, with the Stefan Boltzmann coefficient σ, a wall emissivity ε_w. The body surface emission coefficients ε_{sf} and the view-factors ψ_{sf-w} are listed in table 2 in [2]. D. Fiala uses different values depending on body location and position (sedentary or standing).

2.3.4 Evaporation

The wet heat loss[3], as defined in [1] and [2], through the clothes is driven by the evaporative potential between skin and ambient air

$$Q_{e,cl} = -A_{sk} U^*_{e,cl} (p_{sk} - p_a) \quad (5)$$

Where p_{sk} is the water vapor pressure at the skin, p_a is the vapor pressure of the ambient air, and $U^*_{e,cl}$ is the resultant evaporative heat transfer coefficient. The mathematical relations that define those three functions are not shown here, but can be evaluated from [1], [2] and [5]. Finally the following quantities effect the evaporative heat loss:

- skin temperature: T_{sk}
- ambient air temp., velocity, humidity: T_a , φ_a ,v_a
- local evaporative resistance of the clothes: $R^*_{e,cl}$
- local sweating rate : dm_{sw}/dt

Evaporative heat loss in a hot environment strongly depends on the local sweating rate that can be derived from the global sweating rate SW that is a part of the thermoregulatory response of the active system.

2.4 Finite Element Implementation

To solve the bio heat equation (1), considering the actual set of boundary conditions, a special finite element type has to be established that allows only radial heat conduction. For the radial temperature field we assume a linear function

$$T_e(t,\xi) \approx \sum_{i=1}^{2} T_i^e(t) \cdot \phi_i(\xi) \quad (6)$$

separating nodal temperatures T^e_i from the spatial approximation functions:

$$\phi_1 = \frac{1}{2}(1-\xi) \; ; \; \phi_2 = \frac{1}{2}(1+\xi) \quad (7)$$

This simple approach will then be used to model the temperature distribution in a material layer, as shown in Fig. 4 (red line).

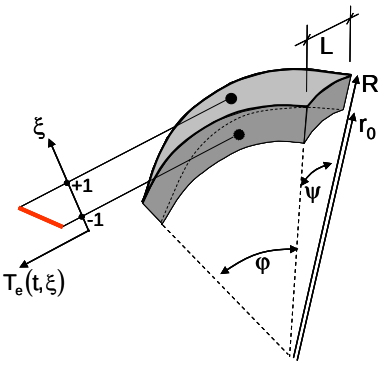

Fig. 4 Geometry of the finite element (FE).

Such finite element might represent a material layer like fat, skin or bone with a linear temperature approach. Or a set of such finite elements might build up one single material layer, as shown for the muscle layer in Fig. 2. Using more than one finite element per layer deals with the fact that in most cases transient loading and inner heat sources result in a nonlinear temperature distribution, as shown in Fig. 5.

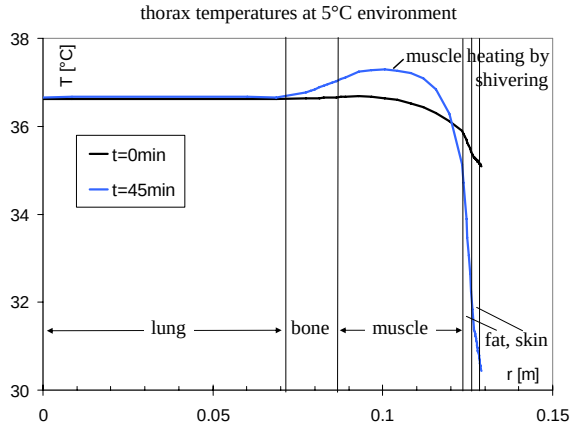

Fig. 5 Radial Temperature Distribution.

A larger number of sub-layers (FE) must be chosen to build up the muscle temperature distribution in such a smooth way as shown in the figure above. The maximum number of sub-layers is limited to 9 in THESEUS-FE today.

Replacing the temperature T in (1) by the simple linear approach (2) and integrating over the finite element's solid region while multiplying with ϕ_i one

[3] always negative values

can show that after some mathematical operations[4] a time differential equation system[5] can be derived, that holds for one single finite element 'e':

$$\underline{M}^e \dot{\underline{T}}^e + \underline{K}^e \underline{T}^e = \underline{Q}^e + \underline{q}^e \tag{8}$$

with

$$M_{ij}^e = a\int_{-1}^{1} \rho c \phi_i^e \phi_i^e r^\omega d\xi \;\; ; \;\; Q_i^e = a\int_{-1}^{1} \phi_i^e (Q_m + \beta T_{bla}) r^\omega d\xi \tag{9}$$

$$K_{ij}^e = d\int_{-1}^{1} k \frac{\partial \phi_i^e}{\partial \xi}\frac{\partial \phi_j^e}{\partial \xi} r^\omega d\xi + a\int_{-1}^{1} \beta \phi_i^e \phi_j^e r^\omega d\xi$$

and

$$t = R - r_0 \;\; ; \;\; r = R - t(1-\xi)/2 \tag{10}$$

For cylindrical coordinates (e.g. leg):

$$a = \varphi L t/2 \;\; ; \;\; d = 2\varphi L/t \;\; ; \;\; A = \varphi L R \tag{11}$$

And for spherical coordinates (e.g. head):

$$b = 1 - \cos\theta \;\; ; \;\; a = \varphi b t/2 \;\; ; \;\; d = 2\varphi b/t \;\; ; \;\; A = \varphi b R^2 \tag{12}$$

The sum over all boundary heat flux densities Σq_{bc} from convection, radiation, evaporation or contact will be integrated on the outer skin (or cloth) layer:

$$q_i^e = A\phi_i^e \sum q_{bc} \quad \text{for } \xi = 1 \tag{13}$$

3 Fiala's Active System

The active system controls regulatory responses of shivering, sweating and peripheral vasomotion in terms of global manikin functions depending on three state variables:

- the mean skin temperature: $T_{sk,m}$
- the hypothalamus (head core) temperature: T_{hy}
- and derivations of the mean skin temperature versus time: $dT_{sk,m}/dt$

The non-linear active system function in [1] and [3] had been derived from regression analysis, taking into account a huge number of test cases. A detailed description of the manikin's active system (with its influences on the passive system) can be found in literature and will not be shown here.

4 Validation

In his PhD thesis [1] D. Fiala collected a large number of experiments from literature where humans had been exposed to different (and changing) environmental conditions. An extensive validation program showed the applicability of his thermal manikin.

In Fig. 6 one single thermal load case is presented that shows the global evaporative response of manikin(s) on hot environmental conditions. The effect of rising evaporative heat loss results from sweating, that is one of the active system response functions.

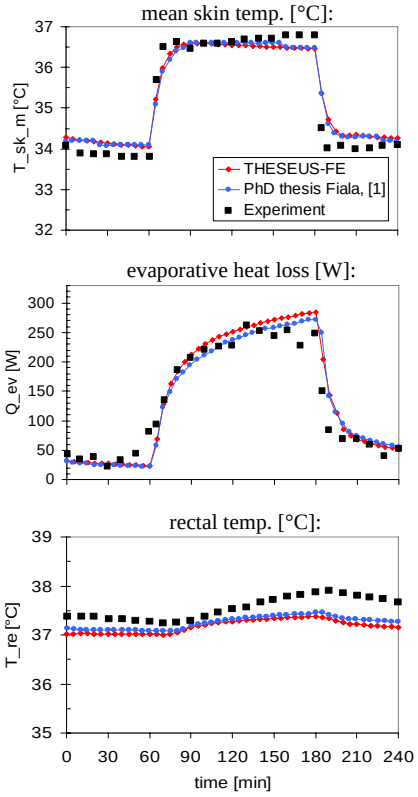

Fig. 6 Human response on a changing environment (28-48-28°C)

Finally a good fit between the THESEUS-FE results and those presented in [1] could be reached. A special manual [6] shows simulation results derived from the new manikin in THESEUS-FE that had been compared with the complete data base in [1].

5 Thermal Comfort

The final purpose of the HVAC (Heating Ventilation and Air Conditioning) –system is to provide comfortable thermal conditions, irrespective of the environmental climatic conditions outside the vehicles cabin. The thermal boundary conditions of the passengers are always time dependent and asymmetric, dominated by convection and radiation. Human discomfort often results from the local appearance of thermal loads hitting body parts with extreme heat fluxes from sun, ventilation or contact.

That's why the prediction of thermal comfort is one of the major aims of thermal simulation today, and especially for vehicle passengers. In THESEUS-FE such manikin simulations typically start from thermal neutrality…

---

[4] E.g. those operations are shown in [4].

[5] The underlined quantities in (8) are vectors or matrices. $\dot{\underline{T}} = \partial \underline{T}/\partial t$.

5.1 Thermal Neutrality

D. Fiala defines the thermal neutrality as a state of optimal thermal comfort at certain boundary conditions

Tab. 1 Boundary Conditions at thermal neutrality

T_a	φ_a	v_a	ε_w	activity
30°C	40%	0.05m/s	0.93	0.8met

Responses from the active system like shivering, sweating and vasomotion do not act at thermal neutrality. Manikin's mean skin and hypothalamus temperature are listed in Tab. 2

Tab. 2 Manikin results [1] at thermal neutrality

$T_{sk,m}$	T_{hy}	Q_{conv}	Q_{rad}	$Q_{e,cl}$
34.4°C	37.0°C	21.5W	38.9W	18.1W

These temperatures typically are used as set-point temperatures for the active system and the thermal comfort prediction. That means that derivations from the set-points lead to active system responses (like sweating and shivering) on the one hand side, and states of discomfort on the other hand site.

Local derivations

$$\Delta T_{sk} = T_{sk} - T_{sk,0} \qquad (14)$$

of the skin temperatures T_{sk} versus their set-point temperatures $T_{sk,0}$ can give the user a first indication for discomfort. In such a context a ΔT_{sk} value of zero represents the optimal state of thermal neutrality for a body element sector.

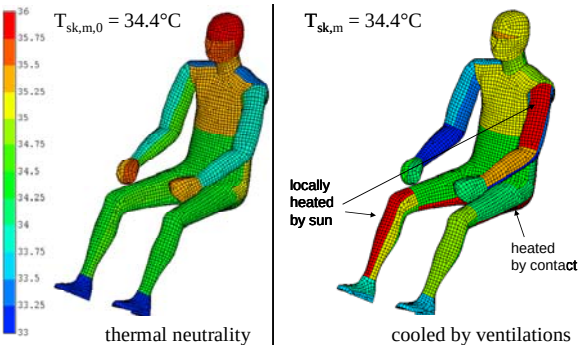

Fig. 7 Skin temperatures at initial and final state of a cabin cool-down simulation with THESEUS-FE

Modern models for thermal comfort prediction will be discussed in the following two sub-chapters: Both models use set-points derivations and some dynamic effects too. That means a proper simulation of the temperatures at thermal neutrality is essentially needed for a later thermal comfort prediction.

5.2 Global Thermal Comfort Prediction (by Fiala)

Fiala's global dynamic thermal sensation index DTS uses set-point derivations of the mean skin temperature and the hypothalamus temperature together with the dynamic variable $dT_{sk,m}/dt$. The three state variables used for the DTS index calculation are the same as for the active system[6].

$$DTS = DTS\left(\Delta T_{sk,m}, \Delta T_{hy}, \dot{T}_{sk,m}\right) \qquad (15)$$

This index runs from -3 (cold) to +3 (hot) and is for many load cases comparable with the well known PMV index[7]. In standard simulations the influence of ΔT_{hy} is quite low and the mean skin temperature derivations affects the DTS index mainly. Relations between $\Delta T_{sk,m}$ and the DTS index are shown in the figure below.

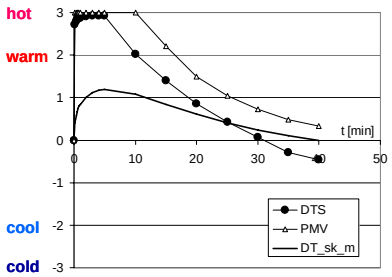

Fig. 8 Global Results from a cool-down simulation.

The manikin skin temperatures are initialized at thermal neutrality (Fig. 7) and the boundary conditions start with very high cabin air and radiation wall temperatures. A sudden rise of skin temperatures makes the DTS index rise up to its maximum value of +3. This dynamic effect results from the third state variable in (15).

After about 5 minutes simulation ventilations (blowing cold air inside the cabin) lead then to falling mean skin temperatures that reach the state of neutrality at 34.4°C after 40 minutes. The dynamic thermal sensation indices shows well-being in a range of -1..+1. Nevertheless a skin temperature distribution as shown in Fig. 7 (right hand side) makes it clear that a certain value for the mean skin temperature often hides information about local asymmetries that might be responsible for local discomfort. See Fig. 7: a cooled right arm and a heated left arm neglect each other in the mean temperature calculation.

Finally there is a strong need for a local thermal comfort model today. Such a model had been presented by Zhang in [7]…

5.3 Local Thermal Comfort Prediction (by Zhang)

As a result of here PhD thesis Zhang presented a very complex mathematical framework for local thermal comfort prediction in [7]. The principle idea of here model is visualized in Fig. 9. At a first step the human hypothalamus and skin temperatures must be derived from measurement or a thermal manikin simulation. In

[6] See chapter 3.

[7] See [8].

a second step local thermal sensation indices can be calculated for certain body parts (e.g. head, face, upper arm). The state variables used therefore are temperature derivations versus neutrality and derivatives with respect to time, as shown in Fig. 9.

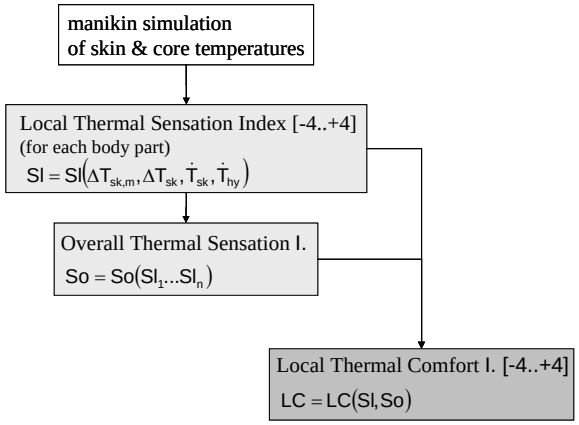

Fig. 9 Zhang's local comfort model.

An overall thermal sensation index can then be found with pre calculated Sl values. Finally the local thermal comfort index is a function of the overall thermal sensation and the related local thermal sensation index of the body part. All these mathematical functions consider a huge number of local weighting factors derived from experiments and regression analysis.

In [10] a method had been presented that shows how one could derive seat temperatures (at the contact area) that would realize a maximum local comfort index at the manikins back. Therefore the workflow shown in Fig. 9 must be reversed, starting with a local comfort index +4 with the final aim to derive contact temperatures that realize this maximum comfort at given boundary conditions. The simple question behind such an analysis is: "what is the optimal contact temperature in a cold vehicle".

5.4 Local Equivalent Temperatures

The principle idea is to take simulated heat fluxes as an input and derive more meaningful temperatures…

In [9] the definition of an equivalent temperature is given: "The equivalent temperature T_{eq} is the temperature of an imaginary enclosure with the same mean radiant temperature and air temperature and zero air velocity in which a person exchanges the same heat loss by convection and radiation as in the actual condition".

This method can be used in a global and a local way. A global way would mean to derive on single value for T_{eq} for a manikin at a certain state of the simulation. A local way would derive equivalent temperatures at each body element sector with known temperatures (skin, cloth) and heat fluxes:

$$\sum Q_{bc} = \frac{A_{sf}\sigma\varepsilon_{sf}\varepsilon_w\psi_{sf-w}\left(T_{eq}^{\ 4} - T_{sf}^{\ 4}\right) + }{A_{sf}\sqrt{a_{nat}\sqrt{\left|T_{eq} - T_{sf}\right|} + a_{frc}v_{a,eff} + a_{mix}}} \quad (16)$$

The left hand side of (14) builds the sum over all boundary heat fluxes from the manikin simulation, as shown in Fig. 3. On the right hand side the equations (3) and (4) build together the heat loss of a certain body part with an imaginary enclosure with $T_{eq}=T_w=T_a$. The effective air speed $v_{a,eff}$ can be replaced by zero or a low value like 0.05m/s. Equation (14) holds for an equivalent temperature prediction at the clothed body part, replacing the cloth temperature T_{sf} by the skin temperature T_{sk} would lead to an equivalent temperature related to the nude body part. For given manikin temperatures and heat fluxes the only unknown in (14) is the equivalent temperature, that could be derived from an iterative scheme like the Newton Method.

The original concept of the equivalent temperature does not consider evaporative heat loss in the imaginary enclosure. Based on a thermal manikin simulation, an extension of the standard method considering (5) on the right hand side of (14) would be easily possible, because all quantities listed in chapter 2.3.4 are given. The relative humidity of the enclosure should then be a pre defined value.

Finally the idea of the 'equivalent temperature' leads to a quite simple-to-use method of assessing local thermal comfort at very complex boundary conditions, typical for a vehicle simulation.

6 References

[1] D. Fiala. Dynamic Simulation of Human Heat Transfer and Thermal Comfort. PhD thesis, De Montfort University, Leicester, 1998.

[2] D. Fiala, K.J. Lomas, M. Stohrer. A computer model of human thermoregulation for a wide range of environmental conditions: The passive system. J.Appl.Physiol, 87:1957-1972, 1999.

[3] D. Fiala, K.J. Lomas, M. Stohrer. Computer prediction of human thermoregulatory and temperature responses to a wide range of environmental conditions. Int.J.Biometeorol 2001

[4] J.N. Reddy, D.K. Gartling. The Finite Element Method in Heat Transfer and Fluid Dynamics (sec. edition). CRC Press LLC, Boca Raton 2000.

[5] THESEUS-FE, Release 2.0, Theory Manual.

[6] THESEUS-FE, Release 2.0, Manikin FIALA-FE Validation Manual.

[7] H. Zhang. Human Thermal Sensation and Comfort in Transient and Non-Uniform Thermal Environments". PhD Thesis, Center for Environmental Design Research (CEDR), University of California at Berkeley, 2003.

[8] P. O. Fanger. Thermal Comfort: Analysis and Application in Environmental Engineering. Danish Tech. Press, Copenhagen, Denmark, 1970.

[9] H. Nilsson, I. Holmer. Definitions and Measure-ments of Equivalent Temperatures. EQUIV Report nr 1, EU-commission Cost contract No SMT4-CT95-2017

[10] S. Paulke. Finite Element based Implementation of Fiala`s Thermal Manikin in THESEUS-FE. VTMS 2007